

Combining N3LO QCD calculations and parton showers for hadronic collision events

Valerio Bertone¹ and Stefan Prestel²

¹*Irfu, CEA, Université Paris-Saclay, 91191, Gif-sur-Yvette, France*

²*Department of Astronomy and Theoretical Physics,
Lund University, S-223 62 Lund, Sweden*

Detailed and precise background predictions are the backbone of large parts of high-energy collider phenomenology. This requires to embed precision QCD calculations into detailed event generators, to produce comprehensive software simulations. Only continued progress in this direction will allow us to exploit the full potential of measurements at the Large Hadron Collider, or at a future Electron-Ion Collider. This work presents a method to combine third-order QCD calculations for hadronic scattering processes with Monte-Carlo event generators, thus enabling a new generation of precision predictions.

I. INTRODUCTION

Measurements at particle colliders aim to provide insights into the fundamental building blocks of physics by juxtaposing experimentally recorded scattering final states with detailed theory simulations. Any deviation from the expectation (based on the Standard Model of particle physics) hints at new research directions.

This “indirect search” strategy relies on sophisticated event generators, which should furnish an accurate model of the scattering dynamics [1]. On top of this, precision predictions have become ever more important, as detailed error budgets are mandatory for reliable comparisons to experimental data. Such predictions are crucial to the LHC phenomenology programme – where new-physics signals have to be lifted from immense QCD backgrounds – as well as future Electron-Ion colliders, where novel QCD phenomena have to be confronted with higher-order QCD calculations within the collinear factorization approximation. These simulations rely on combining high-precision fixed-order (QCD) calculations with parton evolution via all-order parton showering, yielding higher-order event generators.

NLO event generators [2] have become the staple of LHC phenomenology, while NNLO event generators have, albeit still requiring cutting-edge research, become more commonplace [3]. These generators typically require dedicated implementations of higher-order calculations. Thus, methods to enable higher-order event generators should ideally be known when leaps in precision are achieved in fixed-order calculations.

Recent years have seen impressive progress in producing N3LO fixed-order QCD predictions, both at the inclusive [4] and the fully differential level [5–8]. In some cases, these fully-differential results have even been used to supplement resummed predictions for important observables [6–9]. This note offers a method to produce N3LO event generators for processes with incoming hadrons, expanding on the proof-of-principle work [10] concerned with leptonic collisions. The method employs an intuitive “*subtract what you add*” scheme to disentangle fixed-order corrections and parton-shower contributions, up to third order in QCD. The feasibility of an implementation of the method is tested using the controlled environment of a “toy N3LO calculation”¹. Overall, these tests provide abstract arguments for the validity and accuracy of the NNLO+PS method with a numerical verification.

II. N3LO MATCHING

High-precision event generators typically rely on *matching* or *merging* schemes, which first define the desired precision of the simulation (potentially for specific observables), and then provide an algorithmic realization by combining (possibly a set of) precise fixed-order calculations with subsequent parton showering, while ensuring that no terms are double counted. This allows one to improve both on the accuracy of the simulation – by containing a better approximation of (real-emission) multi-particle states compared to showering – and the precision of the simulation by containing exact virtual corrections, thus (hopefully) yielding better control over renormalization scale uncertainties. A successful matching scheme will ensure that all terms up to the desired order are correctly described at fixed order, while all higher-order terms reproduce the parton-shower result. The latter is ambiguous. This note will follow the reasoning and shower accuracy definition of [10], which is based on obtaining a self-consistent calculation

¹ Differential N3LO fixed-order calculations that produce finite-weight *events* have yet to emerge.

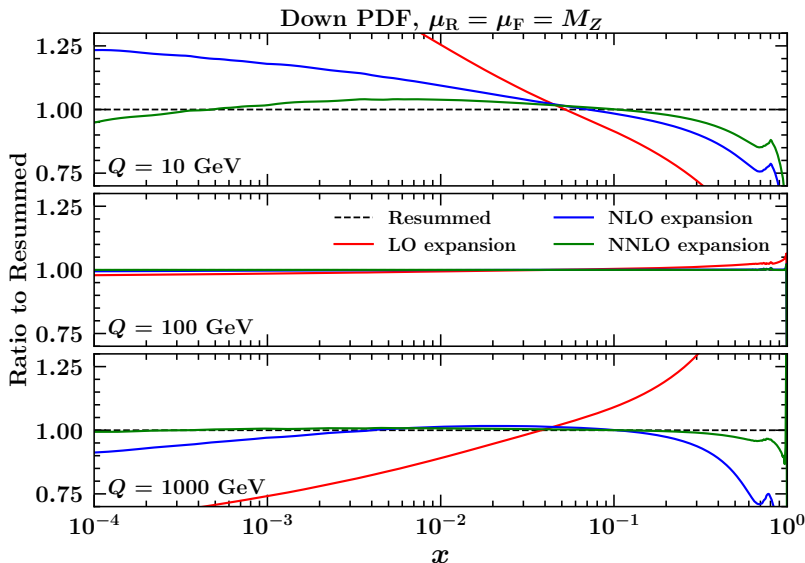


FIG. 1: Comparison of resummed vs. expanded solution of the DGLAP evolution equations. The down-quark PDF as a function of x at three different values of the scale $Q = 10$ GeV (upper plot), 100 GeV (central plot), and 1000 GeV (lower plot) is computed in terms of the PDFs at scale the μ_F and $\alpha_s(\mu_R)$, with $\mu_R = \mu_F = M_Z$, using the resummed solution (dashed black lines) and its expansion to three different orders (see Eqs. (A5)-(A6)): LO (red curves), NLO (blue curves), NNLO (green curves). The curves are presented as ratios to the resummed solution.

without approximating the shower result by an (observable-dependent) log-counting. That being said, we expect the parton-shower (no-emission probabilities) to regularize cross sections of ordered, single-unresolved emissions in the soft and collinear limits.

Typically, the fixed-order and shower regions are regarded as basically complementary. However, very high-precision fixed-order simulations may in fact already provide an approximation of all-order perturbative effects that is – although only an effective description – superior to truly all-order, yet approximate, description of parton showers. One such all-order effect is the evolution of parton distribution functions in initial state showers. Common showering algorithms based on backward evolution e.g. fail to recover DGLAP evolution for long evolution without emission (see contribution titled “Self-consistency of backwards evolved initial-state parton showers” in [11]²). However, already using the (correct) second-order expansion of PDF evolution yields a satisfactory approximation of the all-order result, as shown in Figure 1. Thus, replacing the coefficients of the expansion of the parton shower up to $\mathcal{O}(\alpha_s^2)$ with the correct values will help ameliorate problems with PDF evolution. Only N3LO+PS methods *demand* that the $\mathcal{O}(\alpha_s^2)$ coefficients of the shower be replaced, making hadron-collider extensions of the TOMTE scheme desirable.

The goal of N3LO+PS methods is to provide a unified calculation that retains the relevant fixed-order precision for up to three additional partons throughout all of phase space, while supplementing the fixed-order expansion with all-order effects provided by the parton shower. The accuracy and internal consistency of the parton-shower resummation must not be affected by the matching prescription. Observables that do not require the support of any parton should be described at N3LO precision, observables demanding the presence of at least one parton should be described at NNLO precision, observables mandating two additional final-state partons with NLO precision, and observables depending on at least three additional partons should be predicted with LO accuracy. Whenever any observable is “exclusive”, i.e. relies on a fixed number of final-state jets, all-order effects beyond $\mathcal{O}(\alpha_s^3)$ should be calculated using the parton shower resummation.

A. Basic concepts

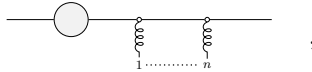
This section aims to introduce the TOMTE method, and illustrate its derivation and most important principles. The original TOMTE publication [10] developed the method in full generality, providing detailed definitions, intermediate

² Methods to overcome such issues have been discussed [12, 13], but require a radical redesign of showering algorithms

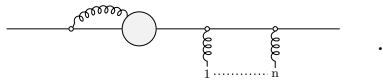
formulae, and somewhat length end results. To complement this discussion, this note will provide a diagrammatic explanation of the method. For this, let us first introduce diagrams that will feature heavily later. The symbol



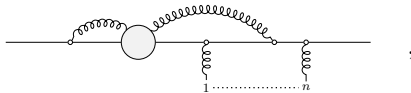
indicates an arbitrary lowest-multiplicity process. Zeroth-order (tree-level) corrections with n additional resolved partons to this process will be illustrated by



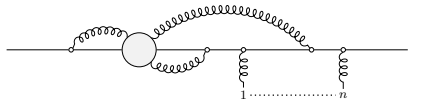
while exclusive first-order (NLO) corrections with n additional partons (comprising one-loop corrections and unresolved real-emission contributions) will be given by



Similarly, exclusive second-order (NNLO) $+n$ -jet corrections will be depicted by



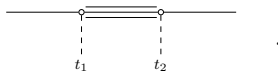
and exclusive third-order (N3LO) $+n$ -jet corrections given by



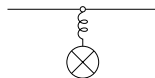
Symbols describing the action of the parton shower include the shower emission vertex



This vertex encapsulates the (higher-order) effect of dynamical renormalization and factorization scale choices for shower emissions at evolution scale t . The probability of not emitting between two shower emissions at scales t_1 and t_2 is symbolized by multiple lines,



Finally, it will be necessary to depict contributions obtained by integrating over the degrees of freedom of one or several final-state particles:



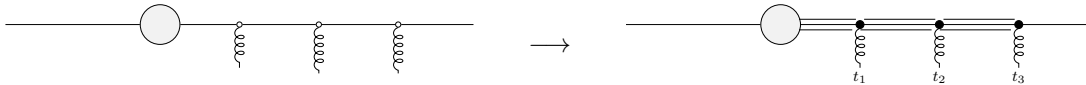
This integration is performed by sampling the full multi-parton phase space, and then projecting the configurations onto the desired multiplicity by choosing an underlying configuration, as first discussed in [14, 15].

When constructing a third-order matched calculation, it will be useful to move from the description of high multiplicity states to that of low multiplicity states, as high-multiplicity states enter as real-emission corrections in lower-multiplicity calculations. Also, the handling of real-emission contributions in the parton shower is directly linked to the generation of no-emission probabilities by virtue of the unitarity of the showering process. In the following, we will (first) discuss the basic concepts of the TOMTE method using the fixed-order contributions starting at $\mathcal{O}(\alpha_s^3)$.

A suitable treatment of the highest possible multiplicity contributions (containing three additional partons relative to the Born process) only requires the comparison of tree-level result $d\sigma_{n+3}^{(0)}(\Phi_{n+3})$ with its parton shower analogon



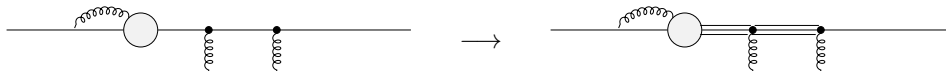
Thus, incorporating all shower higher-order corrections amounts to the replacement



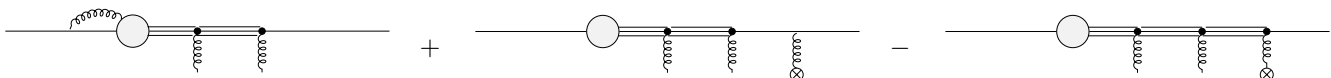
This reweighting requires assigning parton-shower histories (of successive branchings at t_1 , t_2 and t_3) to the $+3$ -parton tree-level phase space points. To guarantee that the all-order description of the shower is not deteriorated, it is important to consider all possible parton shower histories, as discussed at length in [10]. The reweighting is identical to that within the CKKW-L tree-level merging scheme [16, 17]. After the reweighting, the contribution produces, due to the inclusion of no-emission probabilities, a physically meaningful three-jet spectrum, even when partons become (successively) unresolved. As such, it is an appropriate description of the real-emission corrections to Φ_{n+2} states.

The NLO cross section for Φ_{n+2} states consists of tree-level, virtual and real-emission contributions. The latter can be separated into a single-parton unresolved piece (defined here as configurations for which no parton-shower history with three emissions above the shower cut-off ~ 1 GeV can be found) and a resolved component. The former is combined with the virtual corrections into the “exclusive” first-order correction to the Φ_{n+2} rate. This exclusive correction needs to be combined with the resolved real-emission component to obtain the full inclusive NLO correction – whose rate is naively given by the three-parton contributions before reweighting discussed above.

To serve as suitable (N3LO+PS) description of Φ_{n+2} states, any rate has to incorporate the no-emission probabilities to allow partons to become unresolved, and include the effect of the (dynamical) renormalization- and factorization-scale setting mechanism of the parton shower. Thus, the exclusive first-order correction to the Φ_{n+2} is amended with shower all-order factors:



This is the cross section that needs to be complemented with resolved three-parton configurations. At the same time, the three-parton spectrum discussed above should not lead to double-counting, and thus needs to be removed from the inclusive rate. Overall, this means that the contribution to Φ_{n+2} states stemming from fixed-order terms of $\mathcal{O}(\alpha_s^3)$ is given by



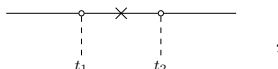
where the second term complements the exclusive cross section, and the third term acts as all-order subtraction of the (reweighted) fully differential three-parton rate.

This discussion highlights the core construction principles of the TOMTE method using exclusive cross sections:

- Create and add a physically meaningful real-emission pattern for m -parton states, by reweighting fixed-order results with appropriate shower all-order factors
- Subtract the real-emission pattern that has been added from the next-lower multiplicity ($m - 1$)
- Create and add a physically meaningful, and appropriate, higher-order exclusive cross section for the $(m - 1)$ -parton states
- Complement the exclusive $(m - 1)$ -parton cross section with an identically-weighted resolved m -parton real-emission pattern; an unbiased inclusive cross section requires the introduction of “bias correction factors” $\mathbf{1}_n^m$ [10].

This yields an $(m - 1)$ -parton matched calculation that may serve as “physically meaningful real-emission pattern” for the next-lower multiplicity $(m - 2)$, and which may be used to iterate the procedure from *b*) onwards, until the minimal multiplicity is reached. The full procedure for contributions with a fixed-order expansion starting at $\mathcal{O}(\alpha_s^3)$ is shown in Figure 2.

Reweightings any contribution starting at $\mathcal{O}(\alpha_s^3)$ will not result change fixed-order coefficients at or below $\mathcal{O}(\alpha_s^3)$, so that the contributions shown in Figure 2 both preserve the precision of the fixed-order prediction and the accuracy of the all-order shower prescription. Any reweighting of contribution starting at $\mathcal{O}(\alpha_s^1)$ or $\mathcal{O}(\alpha_s^2)$ will, however, naively lead to problematic higher-order terms. The reweighting should be appropriately subtracted to avoid this issue. The $\mathcal{O}(\alpha_s^1)$ -term of the no-emission probability will be depicted by



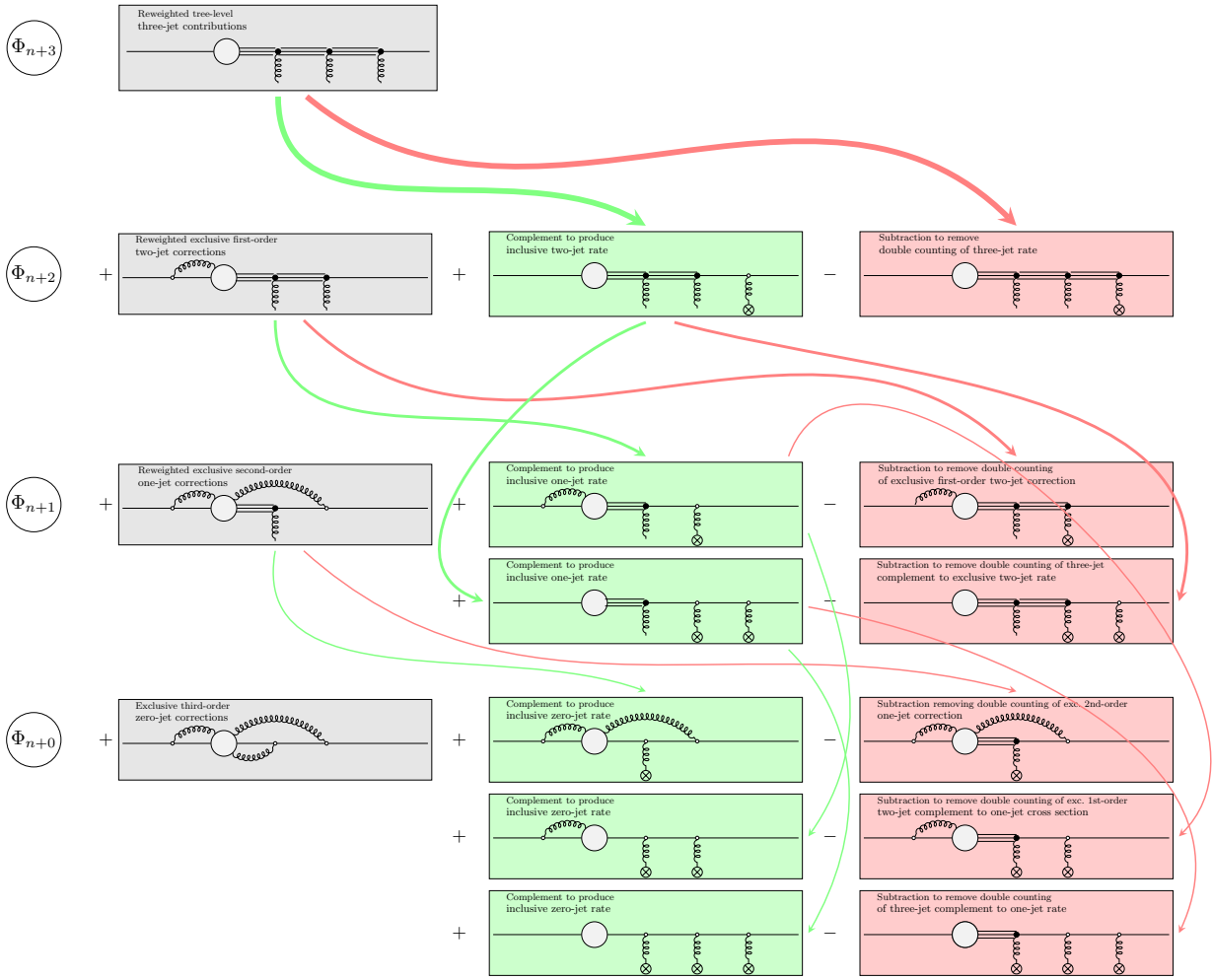
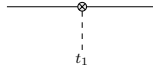


FIG. 2: Diagrammatic representation of the $\mathcal{O}(\alpha_s^{n+3})$ contributions to the TOMTE method. Grey boxes contain (all-order reweighted) fixed-order samples, green boxes complements for exclusive cross sections, and red boxes all-order subtractions to ensure unitarity. The multiplicity of contributions decreases from top to bottom, with the top layer containing Φ_{n+3} phase space points, the next-lower layer Φ_{n+2} , followed by Φ_{n+1} and finally Φ_n phase space points in the bottom layer. Arrows have been added to highlight the relations and/or cancellation between different contributions.

while the $\mathcal{O}(\alpha_s^1)$ -term of the shower vertex is illustrated by



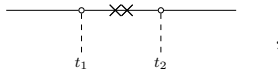
For ease of illustration, it is useful to combine these terms with the all-order no-emission probability and shower vertex to produce an $\mathcal{O}(\alpha_s^1)$ -subtracted parton shower weight. For this, we interpret the product of all all-order factors as a unique weight with a single, common, expansion, and introduce the subtracted weight of Φ_{n+2} states by

$$\begin{aligned}
 & \text{Diagram with vertex and wavy lines} = \text{Diagram with vertex and wavy lines} \\
 & \times \left[1 - \text{Diagram with vertex and wavy lines} - \text{Diagram with vertex and wavy lines} \right. \\
 & \quad \left. - \text{Diagram with vertex and wavy lines} - \text{Diagram with vertex and wavy lines} \right].
 \end{aligned}$$

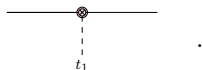
The $\mathcal{O}(\alpha_s^1)$ -subtracted parton shower weight for Φ_{n+1} states is defined analogously as

$$\begin{aligned} \text{Diagram 1} &= \text{Diagram 2} \\ &\times \left[1 - \text{Diagram 3} - \text{Diagram 4} \right] \end{aligned} \quad (1)$$

When reweighting contributions starting at $\mathcal{O}(\alpha_s^1)$, the weight should not contain any $\mathcal{O}(\alpha_s^2)$ terms. Thus, we introduce the diagram



to describe the $\mathcal{O}(\alpha_s^2)$ -term of the no-emission probability, while the $\mathcal{O}(\alpha_s^2)$ -term of the shower vertex is given by



With this, the $\mathcal{O}(\alpha_s^2)$ -subtracted parton shower weight for Φ_{n+1} states is

$$\begin{aligned} \text{Diagram 1} &= \text{Diagram 2} \\ &\times \left[1 - \text{Diagram 3} - \text{Diagram 4} \right. \\ &\quad \left. - \text{Diagram 5} - \text{Diagram 6} + \text{corrections due to eq. 1} \right] \end{aligned}$$

where the “corrections due to eq. 1” remove undesirable $\mathcal{O}(\alpha_s^2)$ terms that are newly introduced by the $\mathcal{O}(\alpha_s^1)$ -subtracted weight defined in eq. 1. Details on the second-order subtracted weight may be found in Appendix A 1.

Using these definitions, the remaining parts of the TOMTE scheme may be constructed. Figure 3 shows the treatment of contributions starting at $\mathcal{O}(\alpha_s^2)$, while Figure 4 illustrates the treatment of terms starting at $\mathcal{O}(\alpha_s^1)$. The TOMTE method then stipulates that

$$\langle O \rangle_{\text{TOMTE}} = \text{Diagram 1} + \text{Figure 4} + \text{Figure 3} + \text{Figure 2}$$

leads to N3LO+PS-correct predictions. The same matching formula in more mathematical detail is given by eq. (24) of [10].

B. Complications for hadronic initial states

When applying the TOMTE method to hadronic collisions, several complications arise relative to its application to leptonic initial states. The previous section introduced the shower all-order weights and their expansions as abstract objects. More concretely, these weights incorporate the effects of *a*) resummation of unresolved emissions for states with large scale hierarchies by means of no-emission probabilities, *b*) dynamical renormalization scale setting for multi-jet processes and *c*) dynamical factorization scale setting in the presence of incoming identified hadrons. Points *a*) and *b*) do already emerge in the discussion of the evolution of $e^+e^- \rightarrow$ jets scattering, and have been discussed in [10]. However, due to the unitarity of the parton-shower evolution, points *a*) and *c*) are linked: The no-emission factors providing the resummation of large scale hierarchies in *a*) contain information about factorization scales, and the about parton distributions. Thus,

- An appropriate reweighting of emission rates includes ratios of PDFs to produce the all-order effects of dynamical factorization scale setting;
- No-emission probabilities will contain exponentiated PDF ratios.

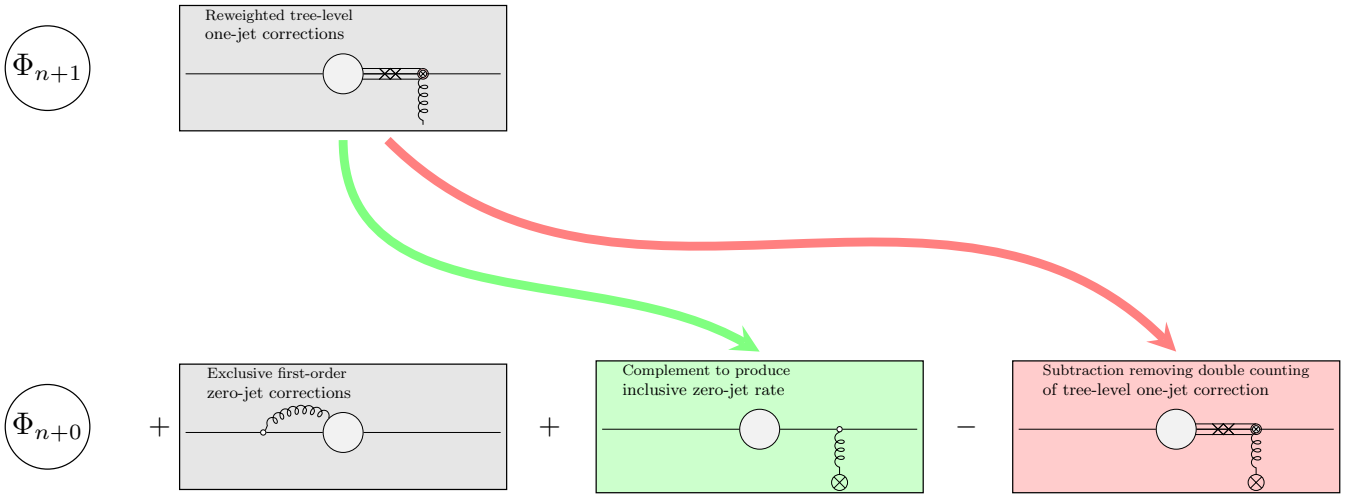


FIG. 4: Diagrammatic representation of the $\mathcal{O}(\alpha_s^{n+1})$ contributions to the TOMTE method. The color coding is identical to that in Figure 3, and as before, the multiplicity of contributions decreases from top to bottom. Arrows have been added to highlight the relations/cancellation between different contributions.

The product of no-emission probabilities and shower vertices provides a suitable all-order reweighting of fixed-order calculations, as e.g. realized in [16, 17] within the context of leading-order merging prescriptions. The product yields the effect of Sudakov resummation when jets become individually unresolved³.

Thus, we will apply the all-order shower weight

$$w_n = \frac{x_n^+ f_{n+}(x_n^+, t_n)}{x_n^+ f_{n+}(x_n^+, \mu_F)} \frac{x_n^- f_{n-}(x_n^-, t_n)}{x_n^- f_{n-}(x_n^-, \mu_F)} \prod_{i=1}^n \left(\frac{x_0^+ f_{0+}(x_0^+, t_{i-1})}{x_0^+ f_{0+}(x_0^+, t_i)} \frac{x_0^- f_{0-}(x_0^-, t_{i-1})}{x_0^- f_{0-}(x_0^-, t_i)} \frac{\alpha_s(t_i)}{\alpha_s(\mu_R)} \right) \Pi_{r_i}(x_i(\Phi_n); t_{i-1}, t_i) \cdot (4)$$

to all fixed-order input for Φ_n , with one or more final-state partons. The \pm indexes the incoming hadrons in with large p^\pm -momentum, and $t_0 = \mu_F$ is used. Whenever the application of this weight induces undesirable behavior at or below $\mathcal{O}(\alpha_s^3)$, the unwanted coefficients in its expansion are removed (by subtraction) to ensure appropriate behavior, as discussed in sec. II A. The presence of PDF ratios makes the order-by-order expansion of the weight cumbersome. The $\mathcal{O}(\alpha_s)$ -coefficient of the expansion of such weights is a necessary ingredient in the UNLOPS NLO merging scheme, and is documented in [23]. However, for N3LO+PS matching, the $\mathcal{O}(\alpha_s^2)$ expansion of this weight is required. The result is somewhat lengthy, and comprises the major complication when applying the TOMTE method to hadronic collisions. All necessary ingredients are presented in Appendix A.

It is important to note that in order to complement the fixed-order cross sections, it is necessary to apply appropriate PDF factors to reclustered complements. If, for example, a three-parton configuration is employed to complement the exclusive one-parton cross section, then the fact that the former has been pre-tabulated with PDFs depending on the initial partons entering in Φ_{n+3} at factorization scale μ_F has to be reflected in the weight. This implies the change

$$\frac{x_n^+ f_{n+}(x_n^+, t_n)}{x_n^+ f_{n+}(x_n^+, \mu_F)} \frac{x_n^- f_{n-}(x_n^-, t_n)}{x_n^- f_{n-}(x_n^-, \mu_F)} \rightarrow \frac{x_n^+ f_{n+}(x_n^+, t_n)}{x_m^+ f_{m+}(x_m^+, \mu_F)} \frac{x_n^- f_{n-}(x_n^-, t_n)}{x_m^- f_{m-}(x_m^-, \mu_F)} \quad (m \geq n), \quad (5)$$

in the first factor in the weight defined in eq. 4. Noting that

$$\frac{x_n^+ f_{n+}(x_n^+, t_n)}{x_m^+ f_{m+}(x_m^+, \mu_F)} \frac{x_n^- f_{n-}(x_n^-, t_n)}{x_m^- f_{m-}(x_m^-, \mu_F)} = \frac{x_n^+ f_{n+}(x_n^+, t_n)}{x_n^+ f_{n+}(x_n^+, \mu_F)} \frac{x_n^- f_{n-}(x_n^-, t_n)}{x_n^- f_{n-}(x_n^-, \mu_F)} \cdot \underbrace{\left(\prod_{i=n+1}^m \frac{x_{i-1}^+ f_{(i-1)+}(x_{i-1}^+, \mu_F)}{x_n^+ f_{n+}(x_n^+, \mu_F)} \frac{x_{i-1}^- f_{(i-1)-}(x_{i-1}^-, \mu_F)}{x_n^- f_{n-}(x_n^-, \mu_F)} \right)}_{w_{m \rightarrow n}^{\text{PDF}}}$$

³ Common transverse-momentum ordered parton showers aim to at least describe leading logarithms for observables linearly related to their evolution variable. Since parton showers include several (semi-)universal effects beyond leading logarithm, the description is, in practise, superior to lowest-order analytic calculations. An accurate log-counting for the parton shower result of specific observables is, however, challenging due to the use of exact kinematics.

offers a simple strategy: The all-order weight applied to complements is given by the original formulation (eq. 4), as is the case for the exclusive counterparts, while the *bias-correction factors* $\mathbb{1}_n^m$ are used to absorb the rescaling $w_{m \rightarrow n}^{\text{PDF}}$.

Finally, high-energy collisions between hadrons feature double- and multiple-parton scattering effects. Naively, the contribution of a secondary QCD interaction arises at $\mathcal{O}(\alpha_s^2)$, and thus warrants a discussion when attempting N3LO+PS matching. Assuming an interleaved multiple interaction paradigm [18, 24] raises the following concerns:

- (1) No-secondary-scattering factors $\Pi_{\text{MPI}}(t_0, t_1)$, containing the probability of no secondary scattering between to scales $t_0 > t_1$, need to be considered;
- (2) Radiation patterns change at $\mathcal{O}(\alpha_s^2)$ and higher, when adding secondary interactions to the LO and NLO contributions of zero-parton configurations Φ_n ;
- (3) Hard secondary scatterings change the available longitudinal momentum left in the colliding hadrons, and thus the PDF factors applied to subsequent radiation from the primary hard scattering.

The no-secondary-scattering factors are given by

$$\Pi_{\text{MPI}}(t_0, t_1) = \exp \left(- \int_{t_1}^{t_0} d\sigma_{\text{MPI}} \right) = 1 - \int_{t_1}^{t_0} \overbrace{d\sigma_{\text{MPI}}(\mu_R, \mu_F)}^{\mathcal{O}(\alpha_s^2)} + \mathcal{O}(\alpha_s^3),$$

where $d\sigma_{\text{MPI}}$ is an appropriately normalized and regularized QCD $2 \rightarrow 2$ scattering cross section. Thus, the application of no-secondary-scattering factors introduces changes at $\mathcal{O}(\alpha_s^2)$. This implies that if the reweighting of one-parton contributions includes no-secondary-scattering factors $\Pi_{\text{MPI}}(t_0, t_1)$, then the tree-level contribution to one-parton states should instead be reweighted by the subtracted no-secondary-scattering factors⁴

$$\Pi_{\text{MPI}}(t_0, t_1) \cdot \left(1 - \int_{t_1}^{t_0} d\sigma_{\text{MPI}}(\mu_R, \mu_F) \right).$$

This shift ensures that only terms of $\mathcal{O}(\alpha_s^4)$ would be introduced by including no-secondary-scattering factors, thus addressing concern (1) above.

Concern (2) could be handled similarly, since a probability of the first secondary scattering instance occurring at a scale t_1 also contains the probability $\Pi_{\text{MPI}}(t_0, t_1)$ of not producing a harder secondary scattering. This latter probability could be subtracted, thus pushing the impact of secondary scatterings on the radiation pattern to $\mathcal{O}(\alpha_s^4)$. However, also without any subtraction, it is worth noting that the double-radiation states introduced by an NNLO calculation ($2 \rightarrow n+2$) have a different structure than those containing a secondary scattering ($2+2 \rightarrow n+2$). If the different states could be disentangled, there would not be any overlap between the calculations, and no subtraction would be necessary. Thus, it appears that concern (2) is best investigated on an observable-by-observable basis.

Finally, concern (3) first arises for states with three final-state partons. We may suggestively write a parton distribution after a secondary scattering as

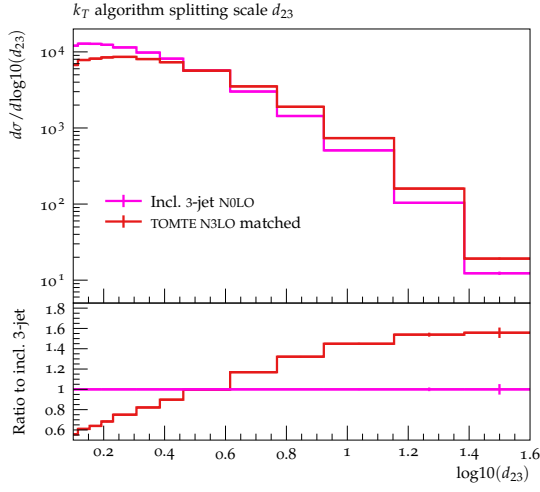
$$f_{\text{MPI}}(x, \mu) = f(x, \mu) + \left[f_{\text{MPI}}(x, \mu) - f(x, \mu) \right].$$

Since secondary scatterings are a higher-order effect, it is reasonable to expect the difference $[f_{\text{MPI}}(x, \mu) - f(x, \mu)]$ to also be an effect beyond $\mathcal{O}(1)$. This is sufficient to ensure that the change in PDF, which could first manifests for states Φ_{n+3} , would not affect the accuracy of the TOMTE method.

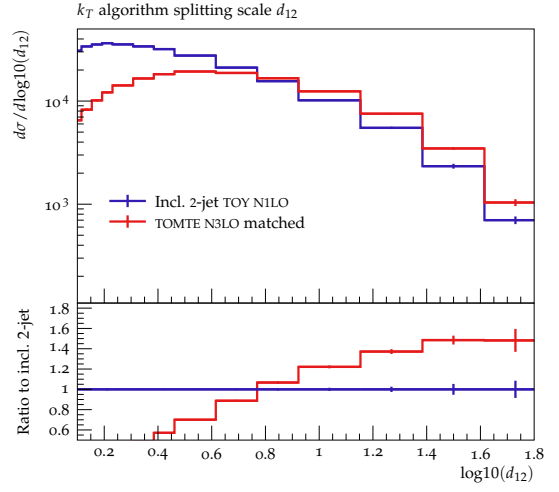
III. CLOSURE TEST WITH DRELL-YAN TOY N3LO CALCULATION

No N3LO fixed-order *event* generators are currently publicly available – not least owing to the fact that a prescription to generate *events* (i.e. unique phase-space points with a bounded contribution to the cross section) typically relies on an N^kLO+PS method allowing a “modified” subtraction of infrared singularities [2, 26] that allows to treat Born-like and radiative phase space regions independently. The validation of a new matching development does, however, rely

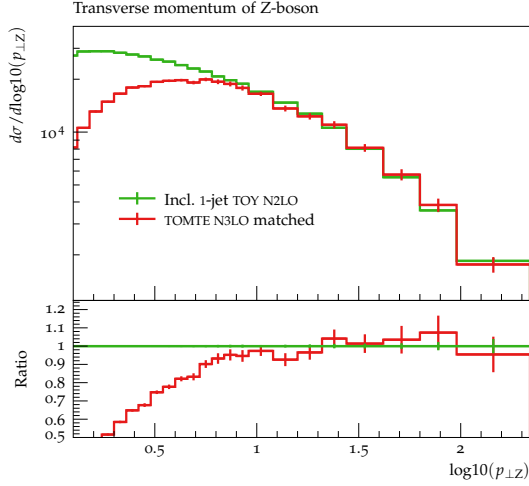
⁴ The terms in parentheses can be generated by applying trial shower methods to secondary scattering proposals.



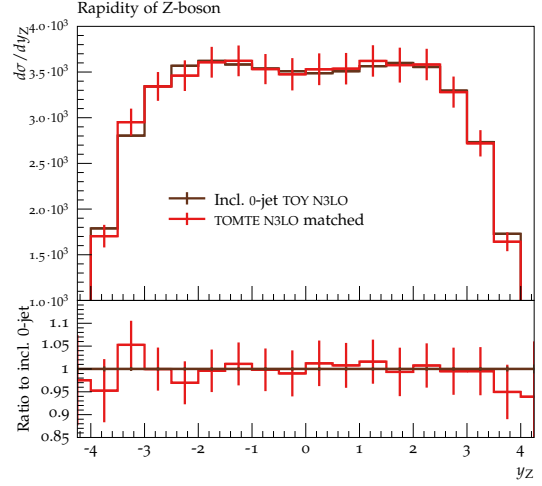
(a) Separation of the 3rd hardest and 2nd hardest jets, as proxy for (inclusive) observables depending on at least three final-state partons.



(b) Separation of the 2nd hardest and hardest jets, as proxy for (inclusive) observables depending on at least two final-state partons.



(c) Transverse momentum of the Drell-Yan pair, as proxy for (inclusive) observables depending on at least one jet.



(d) Rapidity of the Drell-Yan pair, as proxy for observables that are fully inclusive w.r.t. QCD radiation.

FIG. 5: Comparison of toy fixed-order curves and TOMTE results for Drell-Yan lepton-pair production in hadron-hadron collisions. All plots have been produced with RIVET [25]. Bars denote statistical errors.

on appropriate fixed-order events. As argued in [10], this cyclic reasoning can be overcome by validating the N3LO+PS method with “toy calculations”. The construction of such toy calculations should not introduce a dependence on other matching schemes. The toy calculation serves to perform a closure test of (an implementation of) the TOMTE method, i.e. to assess if the matched calculation recovers fixed-order results appropriately in the relevant phase space regions, and yields appropriately resummed results when approaching unresolved limits. Thus, the toy calculations should exhibit typical features of higher-order calculations, yet exaggerate higher-order effects to allow for conclusive validation. This note employs the strategy outlined in [10], with the adjustments outlined in Appendix B to make the method applicable to Drell-Yan lepton pair production in proton-proton collisions.

The MADGRAPH5_aMC@NLO event generator is employed to generate leading-order events for $u\bar{u} \rightarrow e^+e^- + 0, 1, 2, 3$ gluons, which are then used to construct the toy N3LO calculation. We restrict the calculation to $m_{e^+e^-} = M_Z = 91.2$ GeV. Proton-proton collisions are generated at $E_{\text{CM}} = 14$ TeV. The MMHT 2014 LO PDF fit [27], interfaced using LHADPF [28], provides the parton distributions, as well as the α_s reference value, running and flavor thresholds, throughout all aspects of the calculation. Reliable and efficient PDF expansions are provided by the APFEL++ evolution library [29, 30]. The matching is performed using the DIRE shower framework [21] interfaced with the PYTHIA 8.2 event generator [31]. Hadronization and multiple scattering effects have, for the sake of a consistent closure test, been

omitted in the results shown in Figure 5. All code to produce the inputs as well as TOMTE matched results is publicly available at <https://gitlab.com/n3lops/tomte>.

Sample results of the closure test are shown in Figure 5. The “inclusive” results indicate fixed-order predictions, determined from a separate calculation for each panel 5a, 5b, 5c and 5d. All TOMTE results are obtained from a single unified event generation.

The description of inclusive three-parton observables is illustrated by Figure 5a, showing the separation of second- and third-hardest jets in the k_{\perp} jet clustering algorithm [32]. This verifies that the TOMTE prediction provides the expected Sudakov suppression when approaching the limit of the third jet becoming unresolved $d_{23} \rightarrow 0$. The TOMTE prediction overshoots the reference calculation in the well-separated (LO) region. This can be explained by the dynamical renormalization scale choice in the TOMTE prediction, which is inherited from the parton shower prediction. The renormalization scales t_i in the parton shower obey $M_Z^2 = t_0 > t_1 > t_2 > \dots > t_n$, and thus lead to systematically larger α_s values which become ever more apparent with increasing multiplicity. It would appear natural to reaffirm this claim by (artificially) fixing the renormalization scale. That will highlight that the dynamical factorization scale used in parton showers (and hence TOMTE) also has a smaller, but still non-negligible impact. Whereas it is possible to fix the renormalization scale, fixing the factorization scale leads to an inconsistent initial-state shower evolution – unless no-emission probabilities are also omitted. Fixing all these components would lead to an uninteresting, trivial, cross-check. In conclusion, the TOMTE prediction can be argued to lead to appropriate fixed-order results in the region of three well-separated jets, even though the deviation from the fixed-scale results is appreciable. The quality of the prediction should ultimately be assessed by confronting it with data.

Similar findings apply to Figure 5b, which contains the separation of the second-hardest and hardest jets. The Sudakov suppression when approaching the one-resolved-jet region is clearly visible. The (NLO) fixed-order region of two well-separated jets is again populated more within TOMTE, as expected from the previous argument. The effect is slightly less pronounced than for the d_{23} distribution – again as expected from the ordering of renormalization scales discussed above.

The Drell-Yan pair transverse momentum spectrum shown in Figure 5c is sensitive to the presence of one or more final-state partons. The observable beautifully shows the benefits of a matched calculation: For small p_{\perp} values, the TOMTE result exhibits the desired all-order resummed regularization, the transition to high p_{\perp} values is smooth, and at high p_{\perp} the fixed-order (NNLO) result is recovered exactly. This exact match is possible since $t_1 \rightarrow M_Z^2$ as p_{\perp} becomes large, i.e. dynamical renormalization and factorization scales alike approach the reference value M_Z^2 .

Finally, the rapidity of the lepton pair (Figure 5d) should not contain any higher orders introduced by (matching to) the parton shower. Indeed the TOMTE prediction recovers the N3LO toy calculation exactly⁵. Together, the comparisons in Figures 5a - 5d verify that the TOMTE method produces N3LO+PS-accurate predictions also for hadron-collider processes.

The TOMTE method combines the rates of Φ_{n+3} , Φ_{n+2} , Φ_{n+1} and Φ_{n+0} phase-space points into a consistent matched calculation. Given the many contributions to the matching formula, it may be amusing to ask: “*Which contributions are really required to adequately describe an inclusive observable?*” An interesting observable in this context is the Drell-Yan rapidity spectrum, which should receive contributions from any final-state parton multiplicity. The result is shown in Figure 6. The contribution from three-partons (upper left) hardly describes the observable. Adding all two-parton terms (upper center) increases the result, though not nearly enough, whereas further supplementing one-parton terms (upper right) overshoots the desired result at central rapidity. Only the combination of all contributions (containing zero up to three final-state partons; lower panel) leads to the correct result. Matching is required, since none of the contributions are individually close to the true distribution.

IV. SUMMARY AND QUESTIONS FOR THE FUTURE

Event generators form the backbone of the present and future high-energy collider program. This is especially true when relying on “indirect searches”, which rely on high-precision event generators. This note extends the TOMTE method to combine N3LO QCD calculations with parton showers to hadronic initial states. The reweighting in the abstract matching formula presented in [10] was updated to allow for initial-state backward evolution and the dynamical factorization scale setting implied by initial-state parton showers. A numerical closure test was performed, yielding promising results: The TOMTE method may be used to produce high-accuracy predictions for relevant LHC processes.

⁵ The size of the statistical error bars may warrant further explanation. The method removes higher-multiplicity contamination from lower-multiplicity inclusive results (by unitarization), a higher degree of cancellation can be expected for lower multiplicities. Assuming a fixed number of pre-calculated fixed-order events for each multiplicity, this leads to a slower statistical convergence for very inclusive measurements such as the rapidity spectrum.

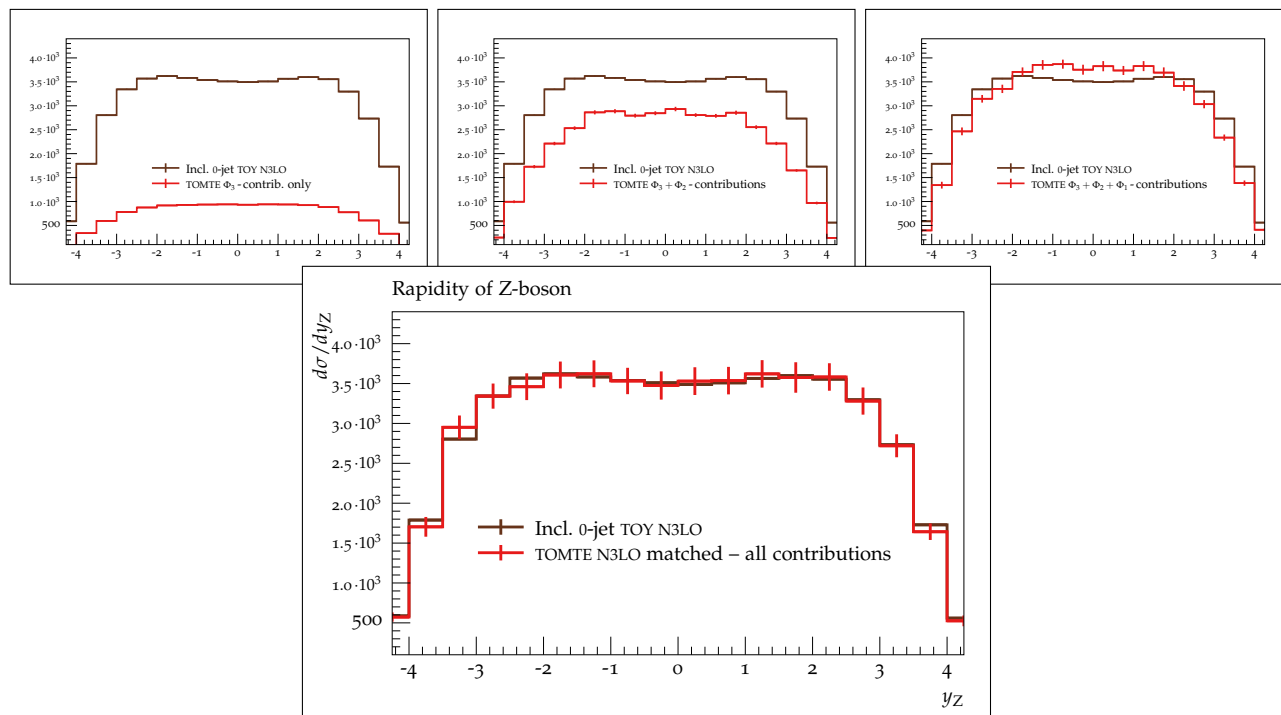


FIG. 6: Comparison of various contributions to the TOMTE matching formula and the baseline toy N3LO results for the Drell-Yan rapidity spectrum.

This is the first proposal for an N3LO+PS method capable of handling incoming hadrons. Thus, ample opportunities for future developments remain. To name a few:

- the treatment of configurations without parton-shower ordering requires detailed agreements between fixed-order calculations and matching frameworks; this statement applies to any matched calculation;
- the handling of secondary or multi-parton scattering phenomena will need to be assessed carefully, both at theoretical and phenomenological level; this becomes pressing already at NNLO+PS level;
- processes with singularities at Born level (such as dijet production at the LHC) may require further developments, such that such singularities are consistently handled in all contributions to the matching formula
- a revised treatment of virtual fixed-order corrections that spreads their effects over higher-multiplicity phase space [3] could lead to results in closer correspondence to analytical resummation, and could be considered

We hope that these questions will inspire future work. The prototype implementation of the TOMTE method used in this publication is publicly available at <https://gitlab.com/n3lops/tomte>.

ACKNOWLEDGEMENT

This note is supported by funding from the Swedish Research Council, contract numbers 2016-05996 and 2020-04303. V. B. is supported by the European Union’s Horizon 2020 research and innovation programme under grant agreement 824093. We thank Stefan Höche for positive encouragement.

Appendix A: Second-order expansions of shower weights

As argued in the original TOMTE publication [10], N3LO+PS matching can be achieved by considering an appropriately reweighted NNLO+PS matched calculation, unitarization, and complementing with an N3LO exclusive (jet-vetoed) cross section. For this strategy to be successful, the main new requirement beyond aspects already present at NNLO is the second-order expansion of the weight applied to tree-level contributions to the rate of one additional final state

parton. The original TOMTE publication was limited to uncolored initial states, in order to avoid having to consider expansions of PDF factors. This is remedied below. In the presence of incoming hadrons, the expansion in $\alpha_s(\mu_R)$ is understood as expansion at fixed μ_F .

1. Problem statement

Overall, we need to find an appropriate subtraction \mathcal{S} such that

$$w_n \left(1 - \frac{\alpha_s}{2\pi} w_n|_1 - \left(\frac{\alpha_s}{2\pi} \right)^2 \mathcal{S} \right), \quad (\text{A1})$$

where w_n is the all-order weight defined in eq. 4, contains $\mathcal{O}(1)$ terms, but no $\mathcal{O}(\alpha_s)$ or $\mathcal{O}(\alpha_s^2)$ terms. All factors should be evaluated at fixed μ_F and fixed μ_R , where applicable.

The weight w_n consists of ratios of all-order factors. In general, using $x = \frac{\alpha_s}{2\pi}$, one may write

$$w \approx \frac{\left[\prod_{i=1}^N a_{i0} \right] \left[\prod_{i=1}^N (1 + x a_{i1} + x^2 a_{i2}) \right]}{\left[\prod_{i=1}^M b_{i0} \right] \left[\prod_{i=1}^M (1 + x b_{i1} + x^2 b_{i2}) \right]}$$

where a_{i0} (b_{i0}) is the zeroth order expansion of one of the numerator (denominator factors), and a_{i1} (b_{i1}) and a_{i2} (b_{i2}) are the first and second-order expansion coefficients, divided by the zeroth-order coefficients, of the numerator (denominator) factors. It is useful to define

$$c_{ij} = \begin{cases} a_{ij} & \text{if } i \leq N \\ -b_{ij} & \text{if } i > N \end{cases}$$

With this,

$$-w|_1 = - \sum_{i=1}^{N+M} c_{i1} \quad (\text{A2})$$

and

$$\begin{aligned} & \frac{\left[\prod_{i=1}^N a_{i0} \right] \left[\prod_{i=1}^N (1 + x a_{i1} + x^2 a_{i2}) \right]}{\left[\prod_{i=1}^M b_{i0} \right] \left[\prod_{i=1}^M (1 + x b_{i1} + x^2 b_{i2}) \right]} \left(1 - x \sum_{i=1}^{N+M} c_{i1} - x^2 \mathcal{S} \right) \\ &= 1 + x^2 \left[\sum_{i=1}^{N+M} c_{i2} - \sum_{i=1}^{N+M} c_{i1} \sum_{j=i}^{N+M} c_{j1} + \sum_{i=1}^M b_{i1}^2 \right] - x^2 \mathcal{S}. \end{aligned}$$

The terms $\propto b_{i1}^2$ arise due to the expansion of denominators. Thus, the subtraction to remove second-order terms is

$$\mathcal{S} = \sum_{i=1}^{N+M} c_{i2} - \sum_{i=1}^{N+M} c_{i1} \sum_{j=i}^{N+M} c_{j1} + \sum_{i=1}^M b_{i1}^2 \quad (\text{A3})$$

To construct this subtraction, the second-order expansion coefficients of all factors in the weight need to be known.

2. Running-coupling expansion

The expansion of $\alpha_s(t)$ in terms of $\alpha_s(\mu_R)$ is straight-forward, and yields

$$\alpha_s(t) = \alpha_s(\mu_R) \left\{ 1 + \frac{\alpha_s(\mu_R)}{2\pi} \beta_0 \ln \left(\frac{\mu_R}{t} \right) + \left[\frac{\alpha_s(\mu_R)}{2\pi} \beta_0 \ln \left(\frac{\mu_R}{t} \right) \right]^2 + \left[\frac{\alpha_s(\mu_R)}{2\pi} \right]^2 \beta_1 \ln \left(\frac{\mu_R}{t} \right) \right\} \quad (\text{A4})$$

$a_2^{q\bar{q}} = -50,$	$a_2^{qg^1} = 10,$	$a_2^{qg^2} = 50,$	$a_2^{\bar{q}g^1} = 10,$	$a_2^{\bar{q}g^2} = 50,$	$a_2^{gg} = 100$
$a_1^{q\bar{q}} = 50,$	$a_1^{qg} = 50,$	$a_1^{\bar{q}g} = 50,$	$b_1^{q\bar{q}} = 0,$	$b_1^{qg} = -300,$	$b_1^{\bar{q}g} = -300$
$a_0^q = 2,$	$a_0^{\bar{q}} = 10,$	$b_0^q = -100,$	$b_0^{\bar{q}} = -100,$	$c_0^q = 500,$	$c_0^{\bar{q}} = 500$

TABLE I: Values of the coefficients a , b and c used in eqs. 3.2 and 3.4 of [10] and eq. B1 of this manuscript.

with

$$\beta_0 = \frac{11}{6}C_A - \frac{2}{3}N_F T_R \quad , \quad \beta_1 = \frac{17}{6}C_A^2 - \left(\frac{5}{3}C_A + C_F\right) N_F T_R$$

The first-order expansion term will be needed below, as both PDF evolution and no-emission probabilities rely on running-coupling evaluations.

3. PDF expansion

We now move to the second-order expansion of PDF ratios. The strategy will be to extract $\mathcal{O}(\alpha_s^2(\mu_R))$ terms at fixed factorization scale μ_F ⁶. The LO (NLO) DGLAP splitting kernels will be written as $P_{a\leftarrow b}^{(0)}(z)$ ($P_{a\leftarrow b}^{(1)}(z)$).

The second-order expansion of $f_a(x, Q)$ (with Q and μ_F GeV²-valued, and assuming the phase-space limits $C(x)$, typically $C(x) = \{z \geq x \cap z \leq 1\}$) is

$$f(x, Q) = f(x, \mu_F) - \left(\frac{\alpha_s(\mu_R)}{4\pi}\right)^1 \ln\left(\frac{\mu_F}{Q}\right) \int_{C(x)} dz \sum_{b=q,g} P_{a\leftarrow b}^{(0)}(z) \frac{x}{z} f_b\left(\frac{x}{z}, \mu_F\right) \quad (\text{A5})$$

$$- \left(\frac{\alpha_s(\mu_R)}{4\pi}\right)^2 \ln\left(\frac{\mu_F}{Q}\right) \int_{C(x)} dz \sum_{b=q,g} P_{a\leftarrow b}^{(1)}(z) \frac{x}{z} f_b\left(\frac{x}{z}, \mu_F\right) \quad (\text{A6})$$

$$+ \left(\frac{\alpha_s(\mu_R)}{4\pi}\right)^2 \left[\ln\left(\frac{\mu_F}{Q}\right) - 2 \ln\left(\frac{\mu_R}{Q}\right) \right] \beta_0 \int_{C(x)} dz \sum_{b=q,g} P_{a\leftarrow b}^{(0)}(z) \frac{x}{z} f_b\left(\frac{x}{z}, \mu_F\right) + \left(\frac{\alpha_s(\mu_R)}{4\pi}\right)^2 \frac{1}{2} \ln^2\left(\frac{\mu_F}{Q}\right) \int_{C(x)} dz \sum_{b=q,g} P_{a\leftarrow b}^{(0)}(z) \int_{C(x/z)} dz' \sum_{c=q,g} P_{b\leftarrow c}^{(0)}(z') \frac{x}{zz'} f_c\left(\frac{x}{zz'}, \mu_F\right) + \mathcal{O}(\alpha_s^3(\mu_R)).$$

4. No-emission probability expansion

Next, it is necessary to expand the no-emission probabilities to second order. For splittings that do not affect initial-state particles, all details were given in [10]. If a radiating system r_i may induce a splitting $s(r_i)$ that changes a pre-branching initial-state particle $p(s)$, thereby changing it to $p'(s)$, then the no-emission probability $\Pi_{r_i}(x; t_0, t_1)$ will contain the ratio of PDFs with different momentum fraction. The expansion of such ratios is given by

$$\frac{\sum_{s(r_i)} K_{f \rightarrow f'(s)}(z) \frac{x}{z} f_{p'(s)}\left(\frac{x}{z}, \rho\right)}{x f_{p(s)}(x, \rho)} = \sum_{s(r_i)} K_{f \rightarrow f'(s)}(z) \left(\frac{\frac{x}{z} f_{p'(s)}\left(\frac{x}{z}, \mu_F\right)}{x f_{p(s)}(x, \mu_F)} - \frac{\alpha_s(\mu_R)}{4\pi} \ln\left(\frac{\mu_F}{\rho}\right) \frac{\frac{x}{z} f_{p'(s)}\left(\frac{x}{z}, \mu_F\right)}{x f_{p(s)}(x, \mu_F)} \left[\int_{C(x/z)} dz' \frac{\sum_{c=q,g} P_{p'(s)\leftarrow c}^{(0)}(z') \frac{x}{zz'} f_c\left(\frac{x}{zz'}, \mu_F\right)}{\frac{x}{z} f_{p'(s)}\left(\frac{x}{z}, \mu_F\right)} - \int_{C(x)} dz' \frac{\sum_{c=q,g} P_{p(s)\leftarrow c}^{(0)}(z') \frac{x}{z'} f_c\left(\frac{x}{z'}, \mu_F\right)}{x f_{p(s)}(x, \mu_F)} \right] \right)$$

⁶ An efficient pre-calculation of PDF convolutions upon initialization currently limits the implementation to processes with ‘‘constant natural factorization scale’’, and thus does not satisfactorily cover processes like e.g. Deep Inelastic Scattering.

With this, the second-order expansion of a no-emission probability amounts to

$$\begin{aligned} \Pi_{r_i}(x; t_0, t_1) &= 1 \\ &- \int_{t_1}^{t_0} \frac{d\rho}{\rho} \sum_{s(r_i)} \int_{\Omega(s(r_i), \rho)} dz \frac{\alpha_s(\mu_R)}{2\pi} K_{f \rightarrow f'(s)}^{(0)}(z) \frac{\frac{x}{z} f_{p'(s)}(\frac{x}{z}, \mu_F)}{x f_{p(s)}(x, \mu_F)} \end{aligned} \quad (\text{A7})$$

$$\begin{aligned} &- \int_{t_1}^{t_0} \frac{d\rho}{\rho} \sum_{s(r_i)} \int_{\Omega(s(r_i), \rho)} dz \left(\frac{\alpha_s(\mu_R)}{2\pi} \right)^2 K_{f \rightarrow f'(s)}^{(0)}(z) \frac{\frac{x}{z} f_{p'(s)}(\frac{x}{z}, \mu_F)}{x f_{p(s)}(x, \mu_F)} \left[\beta_0 \ln \left(\frac{\mu_R}{t} \right) \right. \\ &\quad \left. - \frac{1}{2} \ln \left(\frac{\mu_F}{\rho} \right) \left\{ \int_{C(x/z)} dz' \frac{\sum_{c=q,g} P_{p'(s) \leftarrow c}^{(0)}(z') \frac{x}{zz'} f_c(\frac{x}{zz'}, \mu_F)}{\frac{x}{z} f_{p'(s)}(\frac{x}{z}, \mu_F)} - \int_{C(x)} dz' \frac{\sum_{c=q,g} P_{p(s) \leftarrow c}^{(0)}(z') \frac{x}{z'} f_c(\frac{x}{z'}, \mu_F)}{x f_{p(s)}(x, \mu_F)} \right\} \right] \\ &- \int_{t_1}^{t_0} \frac{d\rho}{\rho} \sum_{s(r_i)} \int_{\Omega(s(r_i), \rho)} dz \left(\frac{\alpha_s(\mu_R)}{2\pi} \right)^2 \frac{K_{f \rightarrow f'(s)}^{(1)}(z) \frac{x}{z} f_{p'(s)}(\frac{x}{z}, \mu_F)}{x f_{p(s)}(x, \mu_F)} \\ &+ \frac{1}{2} \left(\frac{\alpha_s(\mu_R)}{2\pi} \right)^2 \left(\int_{t_1}^{t_0} \frac{d\rho}{\rho} \sum_{s(r_i)} \int_{\Omega(s(r_i), \rho)} dz \frac{K_{f \rightarrow f'(s)}^{(0)}(z) \frac{x}{z} f_{p'(s)}(\frac{x}{z}, \mu_F)}{x f_{p(s)}(x, \mu_F)} \right)^2 + \mathcal{O}(\alpha_s^3(\mu_R)) \end{aligned} \quad (\text{A8})$$

This completes the derivation of all ingredients required to construct the second-order subtractions \mathcal{S} of eq. A3.

Appendix B: Constructing a toy calculation for validation

Currently, no N3LO event generators are available. Thus, to test the feasibility and correctness of the TOMTE scheme, ‘‘toy calculations’’ are employed. These calculation are constructed from (minimally regularized) tree-level calculations through reweighting. Although not providing accurate results, this has the benefit that the matched calculation can be validated in detail, since the consequences of (toy) higher-order corrections are known exactly.

The method to produce a toy calculation in [10] almost directly applies to the hadron collider case. The functional form of the N3LO part of the toy calculation is modified to

$$\begin{aligned} d\sigma_0^{(0+1+2+3)[\text{TOY}]}(\Phi_0) &= \left\{ \int d\Phi_0 d\sigma_0^{(0)}(\Phi_0) \cdot \left[1 + \frac{\alpha_s}{2\pi} (a_0^q x_q + a_0^{\bar{q}} x_{\bar{q}}) + \left(\frac{\alpha_s}{2\pi} \right)^2 (b_0^q (1-x_q) \ln x_q + b_0^{\bar{q}} (1-x_{\bar{q}}) \ln x_{\bar{q}}) \right. \right. \\ &\quad \left. \left. + \left(\frac{\alpha_s}{2\pi} \right)^3 (c_0^q x_q \cos 2\pi x_q + c_0^{\bar{q}} x_{\bar{q}} \sin 2\pi x_{\bar{q}}) \right] \right. \\ &\quad \left. - \int d\Phi_1 d\sigma_1^{(0+1+2)[\text{TOY INC}]}(\Phi_1) \right\} \mathcal{O}_0 + \int d\Phi_1 d\sigma_2^{(0+1+2)[\text{TOY INC}, Q(\Phi_1) < Q_c]}(\Phi_1) \mathcal{O}_0, \end{aligned} \quad (\text{B1})$$

where x_q ($x_{\bar{q}}$) is the momentum fraction of the incoming quark (anti-quark). The coefficients of the kinematic modulations (section 3 of [10]) that define all toy calculations are listed in Table I.

The only other additional complication arises due to PDF factors. Approximations for loop integrals are constructed from higher-multiplicity matrix elements. These proxies should be evaluated using parton luminosities applicable to Born phase space points. It is assumed that the same holds for unresolved real-emission corrections. Hence, all contributions to the toy calculation for Φ_n should be evaluated with parton luminosities related to Φ_n . In practise, this is achieved by applying a PDF reweighting to higher-multiplicity events when constructing approximate virtual and (unresolved) real contributions.

-
- [1] A. Buckley *et al.*, Phys. Rept. **504**, 145 (2011), 1101.2599.
[2] S. Frixione and B. R. Webber, JHEP **06**, 029 (2002), hep-ph/0204244.
P. Nason, JHEP **11**, 040 (2004), hep-ph/0409146.
S. Frixione, P. Nason, and C. Oleari, JHEP **11**, 070 (2007), 0709.2092.

- [3] N. Lavesson and L. Lonnblad, *JHEP* **12**, 070 (2008), 0811.2912.
 S. Höche, Y. Li, and S. Prestel, *Phys. Rev.* **D91**, 074015 (2015), 1405.3607.
 S. Höche, Y. Li, and S. Prestel, *Phys. Rev. D* **90**, 054011 (2014), 1407.3773.
 K. Hamilton, P. Nason, E. Re, and G. Zanderighi, *JHEP* **10**, 222 (2013), 1309.0017.
 A. Karlberg, E. Re, and G. Zanderighi, *JHEP* **09**, 134 (2014), 1407.2940.
 K. Hamilton, P. Nason, and G. Zanderighi, *JHEP* **05**, 140 (2015), 1501.04637.
 S. Alioli, C. W. Bauer, C. Berggren, F. J. Tackmann, and J. R. Walsh, *Phys. Rev. D* **92**, 094020 (2015), 1508.01475.
 W. Astill, W. Bizoń, E. Re, and G. Zanderighi, *JHEP* **11**, 157 (2018), 1804.08141.
 S. Höche, S. Kuttimalai, and Y. Li, *Phys. Rev. D* **98**, 114013 (2018), 1809.04192.
 E. Re, M. Wiesemann, and G. Zanderighi, *JHEP* **12**, 121 (2018), 1805.09857.
 P. F. Monni, P. Nason, E. Re, M. Wiesemann, and G. Zanderighi, *JHEP* **05**, 143 (2020), 1908.06987.
 P. F. Monni, E. Re, and M. Wiesemann, *Eur. Phys. J. C* **80**, 1075 (2020), 2006.04133.
 D. Lombardi, M. Wiesemann, and G. Zanderighi, (2020), 2010.10478.
 Y. Hu, C. Sun, X.-M. Shen, and J. Gao, (2021), 2101.08916.
 S. Alioli *et al.*, (2020), 2010.10498.
 J. Mazitelli *et al.*, (2020), 2012.14267.
- [4] C. Anastasiou, C. Duhr, F. Dulat, F. Herzog, and B. Mistlberger, *Phys. Rev. Lett.* **114**, 212001 (2015), 1503.06056.
 C. Duhr, F. Dulat, and B. Mistlberger, *Phys. Rev. Lett.* **125**, 051804 (2020), 1904.09990.
 C. Duhr, F. Dulat, and B. Mistlberger, *Phys. Rev. Lett.* **125**, 172001 (2020), 2001.07717.
 L.-B. Chen, H. T. Li, H.-S. Shao, and J. Wang, *Phys. Lett. B* **803**, 135292 (2020), 1909.06808.
 C. Duhr, F. Dulat, and B. Mistlberger, *JHEP* **11**, 143 (2020), 2007.13313.
- [5] F. Dulat, B. Mistlberger, and A. Pelloni, *JHEP* **01**, 145 (2018), 1710.03016.
 J. Currie *et al.*, *JHEP* **05**, 209 (2018), 1803.09973.
 F. A. Dreyer and A. Karlberg, *Phys. Rev. D* **98**, 114016 (2018), 1811.07906.
 L. Cieri, X. Chen, T. Gehrmann, E. W. N. Glover, and A. Huss, *JHEP* **02**, 096 (2019), 1807.11501.
 R. Mondini, M. Schiavi, and C. Williams, *JHEP* **06**, 079 (2019), 1904.08960.
 X. Chen *et al.*, (2021), 2102.07607.
- [6] G. Billis, B. Dehnadi, M. A. Ebert, J. K. L. Michel, and F. J. Tackmann, (2021), 2102.08039.
- [7] S. Camarda, L. Cieri, and G. Ferrera, (2021), 2103.04974.
- [8] E. Re, L. Rottoli, and P. Torrielli, (2021), 2104.07509.
- [9] A. Banfi *et al.*, *JHEP* **04**, 049 (2016), 1511.02886.
- [10] S. Prestel, *JHEP* **11**, 041 (2021), 2106.03206.
- [11] S. Amoroso *et al.*, Les Houches 2019: Physics at TeV Colliders: Standard Model Working Group Report, in *11th Les Houches Workshop on Physics at TeV Colliders: PhysTeV Les Houches*, 2020, 2003.01700.
- [12] T. D. Gottschalk, *Nucl. Phys. B* **277**, 700 (1986).
- [13] Z. Nagy and D. E. Soper, *Phys. Rev. D* **102**, 014025 (2020), 2002.04125.
- [14] M. Rubin, G. P. Salam, and S. Sapeta, *JHEP* **09**, 084 (2010), 1006.2144.
- [15] L. Lönnblad and S. Prestel, *JHEP* **02**, 094 (2013), 1211.4827.
- [16] L. Lönnblad, *JHEP* **05**, 046 (2002), hep-ph/0112284.
- [17] L. Lönnblad and S. Prestel, *JHEP* **03**, 019 (2012), 1109.4829.
- [18] T. Sjöstrand and P. Z. Skands, *Eur. Phys. J. C* **39**, 129 (2005), hep-ph/0408302.
- [19] S. Schumann and F. Krauss, *JHEP* **03**, 038 (2008), 0709.1027.
- [20] S. Platzer and S. Gieseke, *JHEP* **01**, 024 (2011), 0909.5593.
- [21] S. Höche and S. Prestel, *Eur. Phys. J. C* **75**, 461 (2015), 1506.05057.
- [22] T. Sjöstrand, *Phys. Lett.* **157B**, 321 (1985).
- [23] L. Lönnblad and S. Prestel, *JHEP* **03**, 166 (2013), 1211.7278.
- [24] T. Sjostrand and M. van Zijl, *Phys. Rev. D* **36**, 2019 (1987).
- [25] C. Bierlich *et al.*, *SciPost Phys.* **8**, 026 (2020), 1912.05451.
- [26] S. Hoeche, F. Krauss, M. Schonherr, and F. Siegert, *JHEP* **09**, 049 (2012), 1111.1220.
- [27] L. A. Harland-Lang, A. D. Martin, P. Motylinski, and R. S. Thorne, *Eur. Phys. J. C* **75**, 204 (2015), 1412.3989.
- [28] A. Buckley *et al.*, *Eur. Phys. J. C* **75**, 132 (2015), 1412.7420.
- [29] V. Bertone, S. Carrazza, and J. Rojo, *Comput. Phys. Commun.* **185**, 1647 (2014), 1310.1394.
- [30] V. Bertone, *PoS DIS2017*, 201 (2018), 1708.00911.
- [31] T. Sjöstrand *et al.*, *Comput. Phys. Commun.* **191**, 159 (2015), 1410.3012.
- [32] S. Catani, Y. L. Dokshitzer, M. H. Seymour, and B. R. Webber, *Nucl. Phys. B* **406**, 187 (1993).